Progress In Electromagnetics Research, Vol. 110, 253–266, 2010

FORMULATION OF SCREEN PRINTABLE COBALT NANOPARTICLE INK FOR HIGH FREQUENCY APPLICATIONS

M. Nelo, A. K. Sowpati, V. K. Palukuru, J. Juuti and H. Jantunen

Microelectronics and Materials Physics Laboratories
EMPART Research Group of Infotech Oulu
University of Oulu, P. O. Box 4500, FI-90014, Finland

Abstract—In this work, magnetic metallic cobalt nanoparticles with an average particle size of 28 nm were processed as a dry powder with surface coating material and other organic additives to form a screen-printable ink to be cured at 110°C. EFTEM and TGA-DSC-MS-analyses were used to measure the thickness of the polymer, its coverage on cobalt nanoparticles and the inorganic solid content of the ink. The resolution of the printed patterns and the print quality were evaluated by surface profiler, FESEM and optical microscopy. The relative permeability of the thick film patterns with good printability was measured with a shorted microstrip structure over the frequency range of 0.2 to 4 GHz and complex permeability values were calculated from measured scattering parameter data. The ink attained real part of complex permeability values of up to 5.13 at 200 MHz with 70 wt.% of magnetic filler. The developed ink can be utilized in various printed electronics applications such as antenna substrates and magnetic sensors.

1. INTRODUCTION

Materials with sufficient permeability and permittivity values have wide areas of application in any devices that are used for the manipulation of electromagnetic waves; for example resonators [1], antennas [2], filters [3] and phase shifters [4]. Currently, the electronics industry has a high interest in simple, material and energy saving manufacturing processes using printing methods with a low curing

Received 21 October 2010, Accepted 12 November 2010, Scheduled 20 November 2010
Corresponding author: Mikko Nelo (mikko.nelo@ee.oulu.fi).

temperature. Although feasible nano silver inks are already on the market [5], there is also a need for printable materials with a high permeability, especially for advanced high frequency applications.

Existing materials having high permeability and permittivity values are typically made with high temperature sintering methods or by sputtering [6, 7]. Due to their high temperatures and low throughput these processes are not feasible for all printed electronics manufacturing, for example on organic substrates, and therefore materials with low curing temperatures and suitable electrical properties are needed. An appealing solution is to use ink with a high content of magnetic nanoparticles in order to obtain a material with reasonably high permeability and thus make an ink with good electrical characteristics and printability. This presents an interesting challenge for materials research on printable electronics.

The key issue in the formulation of nanoparticle inks is the stabilization of the particles in suspension. This can be done by adding different surfactants on the surface of the particles, thus making the surface non-polar and more compatible with the organic solvents used in inks. Typical surfactants include organic acids [8] and acid anhydrides, thiols, [9] organic phosphates [10], and polymers with reactive polar functional groups [11, 12]. In order to achieve sufficient mechanical durability, both synthetic products and natural fatty acids are used as binders of the solid components in the printed patterns. In particular, natural fatty acids are an interesting option for binders due to their capability of forming highly cross-linked polymer structures on reaction with atmospheric oxygen. These reactions are catalyzed with transition metals, such as cobalt or zirconium, [13] thus giving an advantage in transition metal based nanoinks compared to synthetic polymers.

In this paper, formulation of screen-printable, low curing temperature ink using magnetic cobalt nanoparticles in dry powder form is investigated. Properties of the realized coating, inks and prints are presented and discussed. Furthermore, magnetic properties of the printed films were characterized with different amounts of solid content using the shorted microstrip transmission-line perturbation (SMTLP) method [14–17] in the frequency range of 0.2 to 4 GHz.

2. EXPERIMENTAL DETAILS

2.1. Materials

Cobalt nanoparticles with an average particle size of 28 nm, (Nanostructured & Amorphous Materials Inc, Los Alamos, USA) and containing 99.8% of cobalt and which were partially passivated with

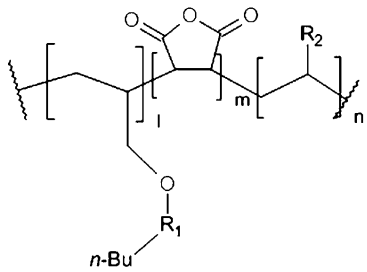

Figure 1. NOF AAB-0851. R_1 = polyethylene oxide, R_2 = Polystyrene.

10% oxygen were used as dry powder in the formulation of the ink. The specific surface area of the powder was 40–60 m^2/g (data supplied by manufacturer) and it was stored in a vacuum bag until 16 h before use. Malialim AAB-0851 surfactant (NOF Co, Tokyo, Japan) was used for the surface treatment of the powder. The polymer consisted of three functional parts (Figure 1) having two side chains where one consisted of polyethylene oxide and the other of polystyrene in order to improve the solubility of the material. The reactive part of the polymer is a carboxylic acid anhydride group forming a covalent bond to the surface of the metal particles. The weight of the repeating unit of the polymer was 968 g/mol and it was calculated from a saponification value given by manufacturer.

Johnson Matthey N 485 (Johnson Matthey Plc, London, UK) was used for adjustment of the rheological properties of the screen-printing ink. The binder and solvents used were Blown Menharden fish oil (Grade Z-3, Richard E. Mistler, Inc, Yardley, USA), xylene (98.5%, ACS reagent grade, Sigma-Aldrich, Germany) and ethanol (99.9%, Aa-grade, Altia, Finland), respectively.

2.2. Ink Formulation

Development of the ink commenced with surface treatment of the Co nanoparticles by applying a solution of AAB-0851 and xylene. The solution was mixed in a ball mill using a nylon pot and agate milling balls. After 16 h of milling, the solution was placed in a furnace and the xylene was evaporated at 80°C for 24 h. The resultant material was analyzed with a LEO 912 OMEGA analytical EFTEM (Carl Zeiss SMT AG, Germany) to characterize the layers of surfactant on top of the particles. Firstly, 0.2 grams of surface treated particles were washed twice with 10 ml of ethanol to remove the excess unreacted polymer

material. The ethanol was vacuum filtered through a 0.2 μm PTFE filter and the particles were collected and dried at room temperature for 24 h before the analysis.

A screen printable base ink was then formed from the surface treated particles. 50 grams of particles, 56 grams of Johnson Matthey N485 solution and 55 grams of ethanol were milled in the ball mill for 24 h to make a smooth paste. Some solvent was then evaporated to increase the viscosity and consistency by using a heating plate and drill mixer. The solids and volatiles of the sample were measured with a Netzsch STA 409PC TGA-DSC-MS (NETZSCH-Geraetebau GmbH, Germany) analyser. Analysis was carried out in a nitrogen atmosphere with a heating rate of 10°C/min. The viscosity of the ink was evaluated at room temperature with a cone and plate rotation rheometer (Bohlin CS, Bohlin rheologi AB, Lund, Sweden).

2.3. Printing Tests

Printings were done using two 10 × 10 inch screens with 325 and 230-mesh nylon screen with 16 μm and 30 μm emulsion thicknesses, respectively. The printer was a Speedline Technologies MPM Microflex screen printer (Speedline Technologies, Inc, USA). Prints with different solid content were made both on 50 μm polyethylene terephthalate foil and on 0.5 mm thick silicon wafers in order to prepare samples for further tests. All printed samples were heat-treated at 110°C for 10 minutes in order to evaporate the volatiles. The printability of the ink was tested by screen printing test patterns. During the printing tests, the viscosity of the ink was increased by evaporating the excess solvent until the print quality of the ink was satisfactory. The best results were achieved when the ink contained 25 wt.% of volatiles and 60 wt.% of cobalt and 15 wt.% organic solids. The proportions of the volatiles and solids were determined by gravimetrical analysis from the printed test patterns.

After good printing characteristics of the ink had been achieved, Menharden oil was added in different proportions to increase the amount of binding material. Samples consisting of 50 to 70 wt.% of Co in the solids contents were fabricated. The heat-treated samples were analyzed with optical microscopy to observe the print-quality and the surface profiles of the printed patterns were evaluated with a Dektak 3st surface profiler (Veeco Instruments Inc, USA). Further analyses of the prints were done with a Zeiss ULTRA plus FESEM (Carl Zeiss SMT AG, Germany) in order to inspect the cross-section of the printed layers.

2.4. Microwave Characterisation

Shorted microstrip transmission-line perturbation was used to measure the complex permeability ($\mu_r = \mu_r' - j\mu_r''$) of the cobalt magnetic thick films with various filler loading levels. The schematic layout of the measurement fixture is shown in Figure 2. The microstrip, ground plane and shorted plane were made of copper. One end of the microstrip line was shorted to the ground and other end soldered to a SubMiniature version A (SMA) coaxial connector. In the design, the characteristic impedance of the microstripline was chosen to be 50 Ω to match the test port of the vector network analyzer. The width of the upper strip (w) was 5 mm, the distance between the upper and ground plane (h) was 1 mm and the length of microstrip line was 20 mm. The effective complex permeability (μ_{eff}) of the samples was obtained by measuring the reflection coefficients of the SMTLP.

The S-parameters, S_{11}^{empty}, S_{11}^{sub} and S_{11}^{film} were measured by a vector network analyzer HP 8720 ES, when the measurement fixture was loaded with air, substrate and substrate with magnetic thick film, respectively. The relationship between the experimental S-parameter data and the propagation constants γ_{sub} (substrate), γ_{film} (thin film deposited on the substrate) can be expressed as [17]:

$$\gamma_{sub} = \gamma_0 - \frac{1}{2 \cdot l} \ln \left(\frac{S_{11}^{sub}}{S_{11}^{empty}} \right) \tag{1}$$

$$\gamma_{film} = \gamma_{sub} - \frac{1}{2 \cdot l} \ln \left(\frac{S_{11}^{film}}{S_{11}^{sub}} \right), \tag{2}$$

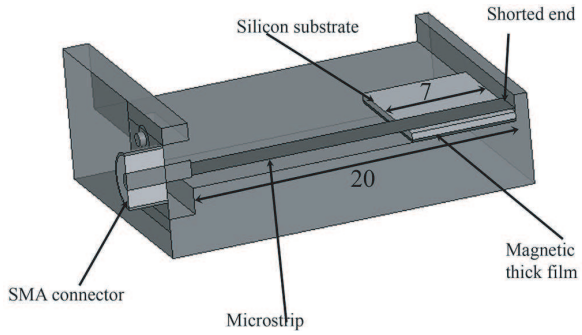

Figure 2. Schematic layout of the shorted microstrip transmission line setup for the magnetic characterization of printed thick films (dimensions in mm).

where is γ_0 the propagation constant of the air-filled microstrip transmission line and l is the length of the sample under test (the value of l equals 7 mm here). The change in the effective permittivity of the multilayered microstrip transmission line caused by the insertion of the thick film was assumed to be negligible [15, 17]. Hence, the effective complex permeability [17] can be obtained as:

$$\mu_{eff} = \left(\frac{\gamma_{film}}{\gamma_{sub}}\right)^2. \tag{3}$$

To extract the complex permeability of the magnetic thick films, conformal mapping was applied to the multilayer microstrip structure [19] shown in Figure 2. After loading the silicon substrate with its printed cobalt magnetic thick film into the fixture, both the effective permittivity and effective permeability of the micro strip transmission line will be changed. The effective permittivity of the multilayer micro strip, can be expressed as [19]:

$$\epsilon_{eff} = 1 - \sum_{i=1}^{3} q_i + \frac{(\sum_{i=1}^{3} q_i)^2}{\sum_{i=1}^{3} \frac{q_i}{\epsilon_{ri}}}, \tag{4}$$

where ϵ_{r1}, ϵ_{r2} and ϵ_{r3} are the relative permittivities of the thick film, substrate and air respectively: q_1, q_2 and q_3 are the filling factors corresponding to the layers and can be calculated from the Equations (5) to (7).

$$q_1 = \frac{h1}{2h} \cdot \left[1 + \frac{\pi}{4} - \frac{h}{w_{eff}} \cdot \ln\left(2w_{eff} \cdot \frac{\sin\frac{\pi h1}{2h}}{h1} + \cos\frac{\pi \cdot h1}{2h}\right)\right] \tag{5}$$

$$q_2 = \frac{h1+h2}{2h} \cdot \left[1 + \frac{\pi}{4} - \frac{h}{w_{eff}} \cdot \ln\left(2w_{eff} \cdot \frac{\sin\frac{\pi h1+h2}{2h}}{h1+h2} + \cos\frac{\pi \cdot h1+h2}{2h}\right)\right] - q_1 \tag{6}$$

$$q_3 = 1 - \frac{h}{w_{eff}} \cdot \ln\left(\frac{\pi w_{eff}}{h} - 1\right) - q_2 - q_1 \tag{7}$$

$$w_{eff} = w + \frac{2h}{\pi} \cdot \ln\left[17.08 \cdot \left(\frac{w}{2h} + 0.92\right)\right] \tag{8}$$

μ_{eff} can be deduced from Equation (4) by using the duality principle [19]

$$\frac{1}{\mu_{eff}} = 1 - \sum_{i=1}^{3} q_i + \frac{(\sum_{i=1}^{3} q_i)^2}{\sum_{i=1}^{3} q_i \mu_{ri}}, \tag{9}$$

where μ_{r1}, μ_{r2} and μ_{r3} are the complex permeabilities of thick film, substrate and air respectively. Then solving the above equation, the

complex permeability of the thick film can be obtained as:

$$\mu_{r1} = \frac{\left[\frac{(\sum_{i=1}^{3} q_i)^2}{\frac{1}{\mu_{eff}} - 1 + \sum_{i=1}^{3} q_i} - q_2 - q_3\right]}{q_1}. \tag{10}$$

3. RESULTS AND DISCUSSION

The particles were analyzed with an EFTEM to ensure the existence of the surfactant layer on the particles. In Figure 3, a 5 nm thick semi-transparent layer of organic material can be seen on the surface of the particles.

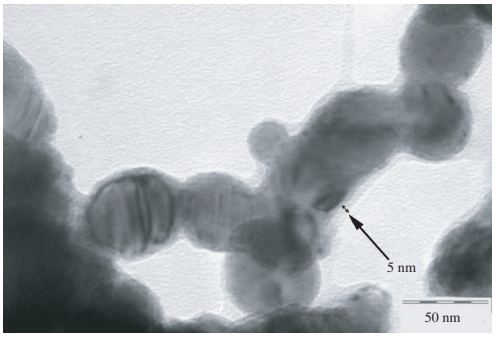

Figure 3. The polymeric layer with a thickness of approximately 5 nm on the surface of the Co particle chains.

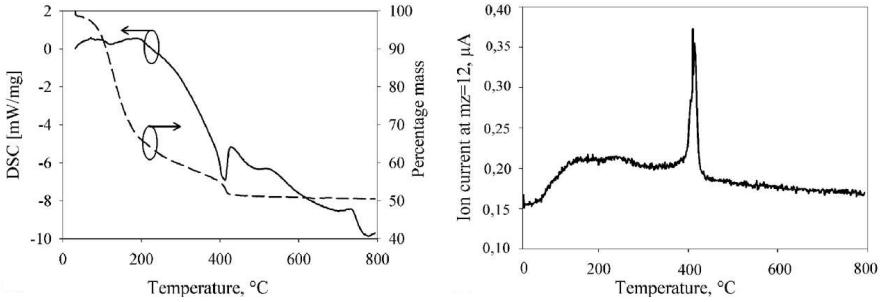

Figure 4. (a) TGA and DSC signals for TG-DSC-MS analysis. (b) MS detector signal indicates the decomposition of solid organic material at 400°C.

The TG-DSC-MS analysis was carried out for the base ink sample before its concentration to printable viscosity. As shown in Figure 4(a), the solvents were first evaporated from the sample after which, at 400°C, the solid organic material decomposes as indicated by the rapid downward peak and decline of the sample weight and calorimetric measurement data. Additionally, Figure 4(b) confirms that the weight loss is caused by decomposition of the organic solids.

The developed ink was analyzed with a cone and plate rotation rheometer, as well as the ink samples which contained Menharden oil to act as a binding material. The change of viscosity caused by the addition of binder material to the samples is shown in Figure 5. Significant decrease in viscosity occurs between the 70 wt.% and 60 wt.% solids samples, which also affected the quality of the printed patterns. Furthermore, the test prints were made with 325 mesh screen to obtain a 10 µm thick dried print layer for magnetic measurements while 230 mesh screen was used for print quality measurements. Print quality tests were carried out by printing 1000, 750, 500 and 250 µm wide parallel lines.

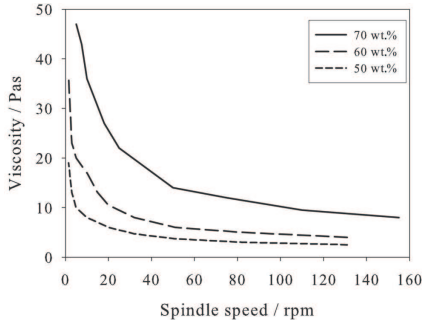

Figure 5. The viscosity of samples with different amounts of cobalt.

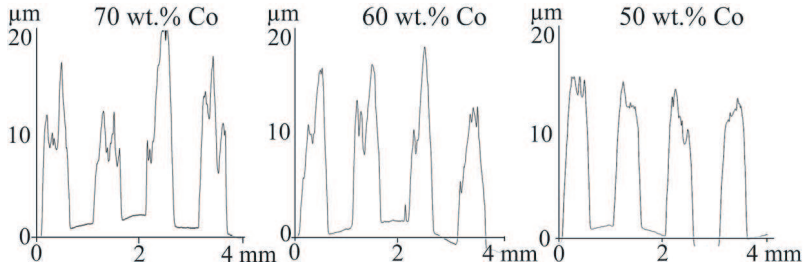

Figure 6. Profiles of the printed patterns containing 70–50 wt.% of cobalt. Lower metal content causes smoother surface and better defined patterns.

The surface profiler analyses of the printed films are presented in Figure 6 for the inks containing 70, 60 and 50 wt.% of cobalt. The results indicate that decreasing the metal content enabled smoother surfaces and better defined printed patterns. However, the amount of particle agglomerates increased when the metal content was reduced, due to the decrease in the viscosity.

Figure 7 shows FESEM images from cross-sections of printed patterns on PET film. The large images are backscattering images taken with a magnification of 1000 x, revealing the location of

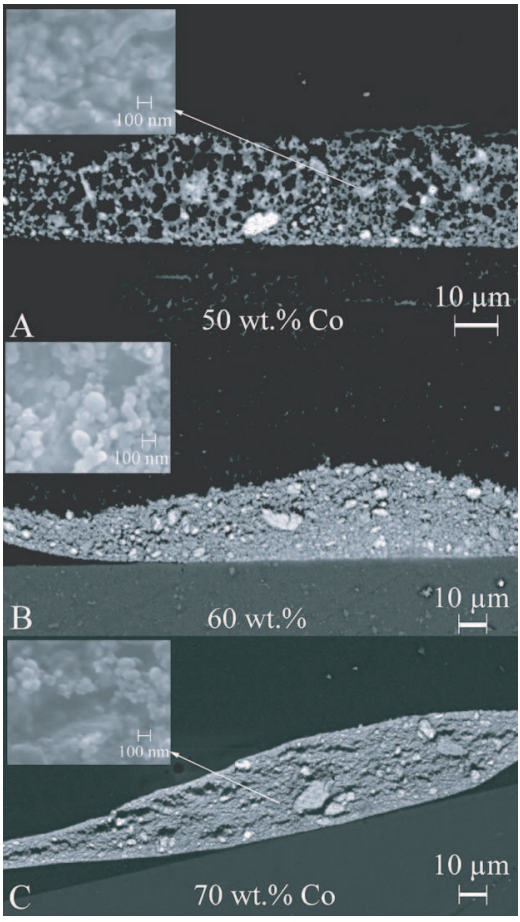

Figure 7. FESEM images of cross-sections of inks printed on PET. Lower magnification (1000 x) images are backscattering images, high magnification (100000 x) are secondary emission images.

the nanoparticles in the printed pattern. These images show that no sedimentation of cobalt occurred during printing. However, agglomeration of the particles can be observed, especially for the sample containing 60 wt.% Co. Cracks in the 70 wt.% sample were caused by the casting process of the SEM samples. The secondary emission images with a magnification of 100000 x (Figure 8, upper left corners) show the nanoparticles in the ink. It can be observed that in the samples containing 60 and 70 wt.% Co the nanoparticles are more visible and also self-arranging in lines, whereas in the 50 wt.% sample the particles are mostly submerged in binding material.

In Figure 8, optical microscopy images of printed 250 µm lines are shown. The measured values for average line widths when printed through 250 µm patterns on the screen were 310 µm, 300 µm and 310 µm for 70 wt.% , 60 wt.% and 50 wt.% Co content, respectively, closely following the differences in viscosity (Figure 6). Furthermore, the size of the agglomerates increased when the metal content was decreased, as shown in Figure 8.

The fabricated shorted microstrip line fixture loaded with a magnetic thick film is shown in Figure 9. Measured real and imaginary parts of the relative permeability of magnetic thick films (μ'_{r1} and μ''_{r1}) with different amounts of filler in the frequency range 0.2 to 4 GHz are shown in Figure 10 and Figure 11. The real part of the permeability (μ'_{r1}) in the frequency region increased with filler loading. The real part of the relative permeability was 5.13, 3.95 and 2.36 at 200 MHz for 70, 60 and 50 wt.% of filler loading, as is shown in Figure 10.

The resonance behaviour observed in the real and imaginary parts of the relative permeability of magnetic thick films with different filler loading levels can be attributed to the inherent ferromagnetic

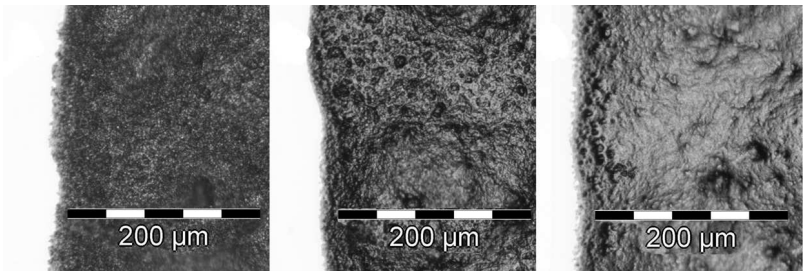

Figure 8. Optical microscopy images of printed patterns, linewidth on screen was 250 µm. (a): 70 wt.%, (b): 60 wt.%, (c): 50 wt.%, cobalt in dry solids.

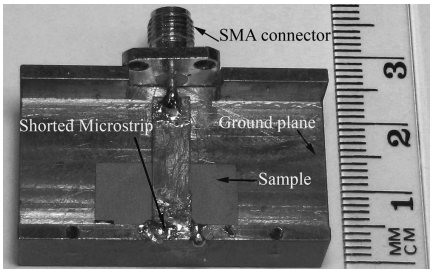

Figure 9. Shorted microstripline fixture loaded with 10 µm thick magnetic film printed on a silicon substrate.

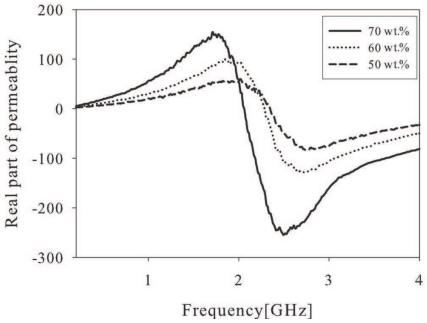

Figure 10. The real part permeability of the printed cobalt magnetic thick films.

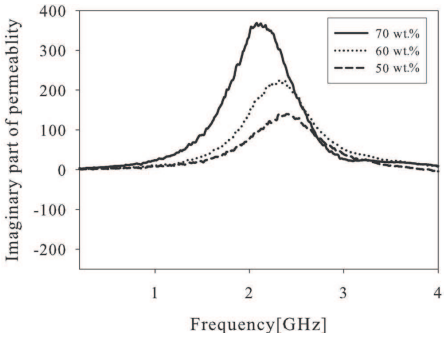

Figure 11. The imaginary part permeability of the printed cobalt magnetic thick films.

resonance (FMR) of the magnetic film. The same phenomenon of FMR in the real and imaginary parts of the relative permeability of thin ferromagnetic films was reported by several authors [15–18]. FMR frequencies of the magnetic thick films were shifted towards lower values with increases in the filler loading levels.

According to the Landau-Lifchitz-Gilbert theory, the ferromagnetic resonance of a magnetic film can be defined as [15]:

$$f_R = \frac{\gamma}{2\pi} \cdot \mu_0 \sqrt{H_S \cdot M_A} \tag{11}$$

where H_S is the saturation magnetic field, M_A is the anisotropic constant, γ is the gyromagnetic ratio.

Further, from constituent relations,

$$B = \mu \cdot H_S \tag{12}$$

Hence, from Equations (11) and (12) one can deduce that,

$$f_R \propto \frac{1}{\sqrt{\mu}}, \tag{13}$$

Thus, the ferromagnetic resonant frequency is inversely proportional to the square root of the magnetic permeability of the magnetic film. With the increase of cobalt filler loading levels in the printed film, the permeability of the film increases, thus the FMR of the film decreases. Ferromagnetic resonances of the fixture loaded with the sample were measured at 1.71 GHz, 1.86 GHz and 2 GHz for 70, 60 and 50 wt.% filler loading levels, respectively as shown in Figure 10.

The imaginary part of the relative permeability (μ''_{r1}) (Figure 11) gradually increased with frequency. The peak frequency of the imaginary part shifted towards lower values with increasing filler loading levels. The imaginary part of the permeability was 3.96, 2.10 and 1.64 for 70 wt.% , 60 wt.% and 50 wt.% of filler loading at 200 MHz.

4. CONCLUSION

In this work, magnetic thick films to be utilized in printed electronics were demonstrated to obtain a relatively high permeability. Inks based on powder-form nanoparticles were realized and cured at low temperatures and are thus feasible for use with various organic substrate materials. The most suitable cobalt content in the ink for screen printing was 70 wt.%, providing the best defined line width, best uniformity of the printed pattern and the most homogenous distribution of the particles in the printed patterns as well as the highest permeability.

ACKNOWLEDGMENT

This work was supported by MAGIA project (No. 40147/08) funded by Tekes, NOF Co., Premix Oy, Perlos Oyj and OMG Kokkola Chemicals Oy. The author AS acknowledges the Finnish Foundation for technology promotion, the Riitta and Jorma J. Takanen Foundation for financial support of the work. Author JJ gratefully acknowledges funding of the Academy of Finland (project number 124011) and HJ acknowledges the Academy of Finland.

REFERENCES

1. Ustinov, A. B., V. S. Tiberkevich, V. Pynttäri, R. Mäkinen, J. Hagberg, and H. Jantunen, "Electric field tunable ferrite-ferroelectric hybrid wave microwave resonators: Experiment and theory," *Journal of Applied Physics*, Vol. 100, No. 9, 093905-1–093905-7, 2006.
2. Castro-Vilaro, A. M. and R. A. R. Solis, "Tunable folded-slot antenna with thin film ferroelectric material," *Proceedings of the IEEE International Symposium of Antennas and Propagation*, Vol. 2, 549–552, 2003.
3. Scheele, P., S. Muller, C. Weil, and R. Jakoby, "Phase-shifting coplanar stubline-filter on ferroelectric-thick film," *Proceedings of the 34th European Microwave Conference*, Vol. 3, 1501–1504, 2004.
4. Yeo, K. S. K., W. Hu, M. J. Lancaster, B. Su, and T. W. Button, "Thick film ferroelectric phase shifters using screen printing technology," *Proceedings of the 34th European Microwave Conference*, Vol. 3, 1489–1492, 2004.
5. Suganuma, K., D. Wakuda, M. Hatamura, and K. S. Kim, "Ink jet printing of nano materials and processes for electronics applications," *Proceedings of the International Symposium on High Density Packaging and Microsystem Integration*, 1–4, 2007.
6. Kulkarnia, D. C., U. B. Lonkarb, and V. Puria, "High-frequency permeability and permittivity of $Ni_xZn_{(1-x)}Fe_2O_4$ thick film," *Journal of Magnetism and Magnetic Materials*, Vol. 320, 1844–1848, 2008.
7. Yang, G. M., A. Daigle, M. Liu, O. Obi, S. Stoute, K. Naishadham, and N. X. Sun, "Planar circular loop antennas with self-biased magnetic film loading," *Electronics Letters*, Vol. 44, No. 5, 332–333, 2008.
8. Lan, Q., C. Liu, F. Yang, S. Liu, J. Xu, and D. Sun, "Synthesis of bilayer oleic acid-coated Fe_3O_4 nanoparticles and their application in pH-responsive Pickering emulsions," *Journal of Colloid and Interface Science*, Vol. 310, 260–269, 2007.
9. Chechik, V. and R. M. Crooks, "Monolayers of thiol-terminated dendrimers on the surface of planar and colloidial gold," *Langmuire*, Vol. 15, 6364–6369, 1999.
10. Papirer, E., E. Walter, A. Vidal, and B. Siffert, "Adsorption of stearic acid and diethyl hexyl phosphate on magnetic metallic iron pigments: Electricla curface charging and absorption competition," *Journal of Colloid and Interface Science*, Vol. 187,

529–538, 1997.

11. Papirer, E., E. Walter, A. Vidal, B. Siffert, and H. Jakusch, "Preparation of magnetic inks: Adsorption of macromolecular dispersion agents on magnetic metallic iron pigments and electrical charge formation," *Journal of Colloid and Interface Science*, Vol. 193, 291–299, 1997.
12. Parvina, S., J. Matsuia, E. Satoa, and T. Miyashita, "Side-chain effect on Langmuir and Langmuir-Blodgett film properties of poly (N-alkylmethacrylamide)-coated magnetic nanoparticle," *Journal of Colloid and Interface Science*, Vol. 313, 128–134, 2007.
13. Sailer, R. A. and M. D. Soucek, "Investigation of cobalt drier retardation," *European Polymer Journal*, Vol. 36, 803–811, 2000.
14. Wu, Y., Z.-X. Tang, Y. Xu, and B. Zhang, "Measure the complex permeability of ferromagnetic thin films: Comparison shorted microstrip method with micro strip transmission method," *Progress In Electromagnetic Research Letters*, Vol. 11, 173–181, 2009.
15. Liu, Y., L. Chen, C. Y. Tan, H. J. Liu, and C. K. Ong, "Broadband complex permeability characterization of magnetic thin films using shorted microstrip transmission-line perturbation," *Review of Scientific Instruments*, Vol. 76, 063911.1–063911.8, 2005.
16. Wu, Y., Z.-X. Tang, Y. Xu, B. Zhang, and X. He, "Measuring complex permeability of ferromagnetic thin film upto 10 GHz," *Progress In Electromagnetic Research Letters*, Vol. 9, 139–145, 2009.
17. Wu, Y., Z.-X. Tang, Y. Xu, B. Zhang, and X. He, "A new shorted microstrip method to determine the complex permeability of thin films," *IEEE Transactions on Magnetics*, Vol. 46, 886–888, 2010.
18. De Cos, D., A. Garcia-Arribas, and J. M. Barandiaran, "Ferromagnetic resonance in gigahertz magneto-impedance of multilayer systems," *Journal of Magnetism and Magnetic Materials*, Vol. 304, 218–221, 2006.
19. Svacina, J, "A simple quasi-static determination of basic parameters of multilayer microstrip and coplanar waveguide," *IEEE Microwave and Guided Wave Letters*, Vol. 2, 385–387, 1992.